



## Purification of alginate improves its biocompatibility and eliminates cytotoxicity in matrix for bone tissue engineering

M.L. Torres<sup>a</sup>, J.M. Fernandez<sup>a,b</sup>, F.G. Dellatorre<sup>c,d</sup>, A.M. Cortizo<sup>a,b</sup>, T.G. Oberti<sup>e,\*</sup>

<sup>a</sup> Laboratorio de Investigaciones en Osteopatías y Metabolismo Mineral, Facultad de Ciencias Exactas, Universidad Nacional de La Plata, 47 y 115 (1900), Argentina

<sup>b</sup> Cátedra Bioquímica Patológica, Facultad de Ciencias Exactas, Universidad Nacional de La Plata, 47 y 115 (1900), Argentina

<sup>c</sup> Centro para el Estudio de los Sistemas Marinos (CESIMAR), CCT CENPAT-CONICET, Bvd. Brown 2915, Puerto Madryn, Chubut, Argentina

<sup>d</sup> Grupo de Investigación y Desarrollo Tecnológico en Acuicultura y Pesca (GIDTAP), Facultad Regional Chubut, UTN, Av. del Trabajo 1536, Puerto Madryn, Chubut, Argentina

<sup>e</sup> Instituto de Investigaciones Físicoquímicas Teóricas y Aplicadas (INIFTA), Facultad de Ciencias Exactas, UNLP, CONICET, CCT, Sucursal 4 Casilla de Correo 16, 1900 La Plata, Argentina

### ARTICLE INFO

#### Keywords:

Sodium alginate  
Structural characterization  
Purification  
Biocompatibility  
Cytotoxicity

### ABSTRACT

There is a growing interest about using natural polymers from renewable sources as biomaterials for applications in tissue engineering. In the present work, alginates were extracted from *Undaria pinnatifida*, a brown sea weed invasive in Argentinian coast. The isolated alginate was structurally characterized by IR and <sup>1</sup>H NMR spectroscopies, intrinsic viscosity and TGA. For comparison purposes, commercial sodium alginate was purified and characterized using the same protocol as for raw material. Toxicity and biocompatibility of sodium alginate obtained from algae were studied using a murine macrophage-like cell line (RAW 264.7) and bone marrow stromal cells (BMSC), respectively. The presence of impurities inhibited both RAW 264.7 and bone marrow stromal cell proliferation and increased nitric oxide production from macrophages, while inhibited osteoblastic differentiation of BMSC. All these effects were reverted by the purification of alginate. In conclusion, alginate purification improves biocompatibility and osteo-induction while decreases its toxicity.

### 1. Introduction

Bone has the ability to repair itself [1], but there are many situations (tumors, osteonecrosis, big fractures) where this capacity cannot overcome the damage caused [2]. Currently, different therapies are used for the treatment of extended bone lesions, among the most frequently used are metal prosthesis and bone grafts. However, both of them present disadvantages that limit its application. In the case of metal prosthesis, there is a lack of remodeling and low osseointegration after implantation. On the other hand, there are two main strategies to obtain bone graft: samples from the patient himself (autograft) and from cadaveric donors (allograft). The main disadvantages of autograft are limited size of the implant and increased morbidity, while for allograft, the disadvantages are disease transmission and reject of the implant by the immune system [3]. In an effort to avoid these disadvantages, tissue engineering combine concepts of different areas (i.e. engineering, medicine, materials science, biochemistry) developing scaffolds to improve bone tissue restoration [4]. In this sense, a large number of materials based on polymers (both natural and synthetic),

ceramics and bioactive glasses are being studied for application in bone tissue engineering [5]. Alginates are a family of linear polysaccharides with  $\beta$ -D-mannuronate (M) and its C-5 epimer  $\alpha$ -L-guluronate (G) units covalently linked together in different sequences or blocks, which can be isolated from natural sources as many brown seaweeds species. *Undaria pinnatifida* (Harvey) Suringar (Ochrophyta, Laminariales) is a brown seaweed species native of Japan, China and Korea, where it is intensively cultivated for human consumption. Recently, this alga has invaded several temperate-cold regions of the world, including the Mediterranean and Atlantic coasts of Europe, Tasmania and south coast of Australia, New Zealand, the Pacific Coast of North America and the Atlantic Coast of South America [6,7]. The first record of this species on the Argentinian coasts was in 1992, in Golfo Nuevo (Chubut), increasing its distribution rapidly all over the coast of Patagonia, and, at present, extending it along most of the Argentine Coast [6]. In Golfo Nuevo, it forms dense seasonal kelp beds that can reach densities over 5 kg/m<sup>2</sup> of wet biomass, and generates some disturbing shifts in the native community [8]. In this current scenario, it is unlikely that *Undaria pinnatifida* could be eradicated from the coasts of Patagonia.

\* Corresponding author at: Instituto de Investigaciones Físicoquímicas Teóricas y Aplicadas (INIFTA), CONICET\_UNLP, CC 16, Suc 4, La Plata, Argentina.

E-mail addresses: [jmfernandez@biol.unlp.edu.ar](mailto:jmfernandez@biol.unlp.edu.ar) (J.M. Fernandez), [dellator@cenpat-conicet.gob.ar](mailto:dellator@cenpat-conicet.gob.ar) (F.G. Dellatorre), [cortizo@biol.unlp.edu.ar](mailto:cortizo@biol.unlp.edu.ar) (A.M. Cortizo), [toberti@inifta.unlp.edu.ar](mailto:toberti@inifta.unlp.edu.ar) (T.G. Oberti).

<https://doi.org/10.1016/j.algal.2019.101499>

Received 2 October 2018; Received in revised form 1 April 2019; Accepted 5 April 2019

Available online 13 April 2019

2211-9264/ © 2019 Published by Elsevier B.V.

Instead, in an attempt to control the invasion, it should be considered as a high-potential biomass feedstock for food production as well as for phycocolloids (mainly alginate and fucoidan) extraction for the biomedical, food and pharmaceutical industries. In this sense, it is interesting to explore the use of alginate from this invading alga as a raw material for the development of bone scaffolds.

A material to be used in tissue engineering ideally must meet certain requirements around biocompatibility, degradability and absence or low toxicity. Additionally, the candidate material should be accessible and available, with a relative low cost of manufacture. Alginate extracted from *Undaria pinnatifida* fulfills all these last requisites. However, both alginates, commercial and extracted from *brown seaweeds*, contain a large number of impurities, such as proteins, endotoxins and polyphenols, which might lead to an intense host immune response reducing the biocompatibility of the alginate-based scaffolds [9,10].

In the present work, we hypothesized that further purification of alginates may improve biocompatibility and eliminate cytotoxicity. In order to demonstrate our hypothesis, we isolated and characterized sodium alginate from blade and midrib of *Undaria pinnatifida*. We also evaluated the type of impurity present in each sample. In *in-vitro* studies, we also investigated the toxicity and biocompatibility of the extracted alginate using a murine macrophage-like cell line (RAW 264.7) and bone marrow stromal cells (BMSC), respectively. In our study, we also included alginate from commercial source for comparison purposes.

## 2. Experimental section

### 2.1. Materials and methods

#### 2.1.1. Alginate source

For this study, we have used two alginate sources: Commercial Alginate (CA) in its salt form as Sodium Alginate (Sigma Aldrich®, CAS Number 9005-38-3) and alginate extracted from *Undaria pinnatifida* proportioned by JONO®, a small company dedicated to the production of wakame and other algal foods in Patagonia, Argentina. The seaweed fronds were dried according to standard production protocols and separated into the main component tissues, blade and midrib. Then, these materials were milled until 1 mm smaller size.

#### 2.1.2. Alginate extraction

Alginate from *Undaria pinnatifida* was extracted and purified using a similar protocol published elsewhere [11] (Scheme 1, A).

Briefly, one part of the midrib (R) or blade (B) of seaweed was soaked with nine parts of formaldehyde 0.1% overnight with constant stirring to eliminate pigments and polyphenols. After that, a pre-extraction procedure was carried out adding distilled water (20 parts per part of algae) and the solution was brought to pH 4 with a 1 N HCl (Anebra), under constant stirring during 15 min. Seaweed solid was recovered by centrifugation at 3000 r.p.m. for 3 min, repeating this procedure twice.

The extraction was performed adding 100 parts of distilled water per part of seaweed. The solution was brought to pH 10 with 10% (w/v) Na<sub>2</sub>CO<sub>3</sub> (Sigma-Aldrich) under agitation for 2 h at 80 °C. After the alkaline extraction, solubilized sodium alginate was separated from the alkali-insoluble seaweed tissue by centrifugation. Alginate was recovered in solid form by precipitation with a solution of 10% (w/v) CaCl<sub>2</sub> (Sigma-Aldrich). The solid was dissolved with distilled water and 1 N HCl until pH 2, the procedure was repeated two times. Finally, the alginate was precipitated with ethanol at pH 8, adding a solution of 10% (w/v) Na<sub>2</sub>CO<sub>3</sub> under shaking for 1 h. The obtained sodium alginate was initially stored frozen at -4 °C overnight, and then freeze-dried at -40 °C for 72 h.

### 2.2. Alginate purification

The purification protocol was based on the Sevag's method for protein removal [12,13] (Scheme 1, B). Briefly, a 1% solution of alginate in water (Commercial Alginate: CA, midRib Alginate: RA, or Blade Alginate: BA) was vigorously shaken in a mix of chloroform/butanol (Cicarelli) (4:1 volume). The procedure was repeated three times, and the final mixture was centrifuged at 3000 r.p.m. during 20 min and the organic phase was discarded. Alginate solution was alkalized (pH 8) by the addition of 10% Na<sub>2</sub>CO<sub>3</sub> and alginate was precipitated from this solution by the addition of ethanol. The obtained solid was initially stored at -4 °C overnight, and then freeze-dried at -40 °C for 72 h to eliminate the solvent. Finally, sodium alginate was dialyzed to eliminate salts and impurities, for that a 1% sodium alginate solution was introduced in cellulose membrane and dialyzed for 7 days (Cut-off: 14,000, Sigma), after which it was freeze-dried for 72 h.

Then, unpurified (CA, RA, and BA) and purified (PCA, PRA and PBA) alginates were characterized by physico-chemical techniques, cytotoxic and biocompatibility studies.

### 2.3. Physico-chemical characterization

#### 2.3.1. Fourier transform infrared spectroscopy

Aqueous solutions of 0.25% sodium alginate were prepared to obtain films for the spectroscopic studies. Fourier Transform Infrared Spectroscopy (FTIR) spectra of sodium alginates (commercial and extracted, purified or not) - films were recorded on a Shimadzu IRAffinity-1 between 4000 and 400 cm<sup>-1</sup> with a resolution of 4 cm<sup>-1</sup> and 40 scans of accumulation.

#### 2.3.2. Thermogravimetric analysis

Thermal stability of the different alginates was studied by Thermogravimetric analysis (TGA) in order to evaluate the variations in the temperature-mass relationship of the materials. The analysis was carried out under a nitrogen atmosphere (TGA Q500-TA Instruments), with a gas purge at 10 °C/min from room temperature to 800 °C.

#### 2.3.3. Nuclear magnetic resonance analysis

M/G composition of CA, RA and BA purified or not was determined by <sup>1</sup>H NMR spectrometry according to the protocol proposed by Fertah et al. [14]. The measurement was recorded in D<sub>2</sub>O at 85 °C using a Bruker 500 MHz instrument. Chemical shifts are reported relative to water peak.

#### 2.3.4. Viscosity

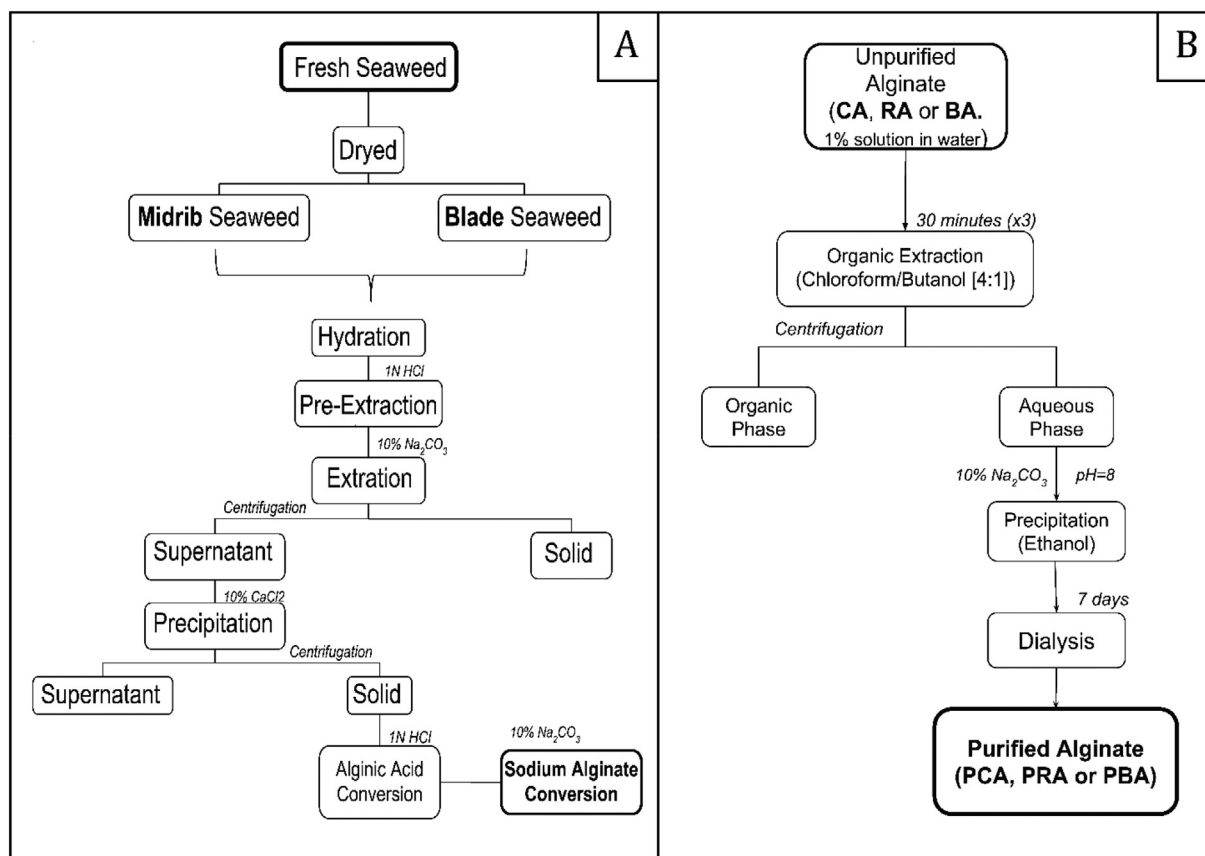
The determination of the intrinsic viscosity ([η]) was carried out by dissolving the different alginate samples in NaCl 0.1 M under mechanical agitation during 24 h, at room temperature.

After that, dilutions from a stock solution, previously filtered with a 0.22 μm membrane, were prepared in NaCl 0.1 M, such that the specific viscosity (η<sub>sp</sub>) was 0.3 < η<sub>sp</sub> < 0.8. Dilutions viscosities were measured with Ostwald capillary viscometer at 20 °C. The viscometric average molecular weight (M<sub>v</sub>) was estimated according to Mark-Houwink equation [15]:

$$[\eta](\text{mL g}^{-1}) = 4.85 \times 10^{-3} M_v^{0.97}$$

#### 2.3.5. Polyphenol determination

The amount of total soluble phenols was determined according to the Folin-Ciocalteu method [16] with slightly modifications. Briefly 100 μL of 1% sodium alginate solutions (CA, RA, BA, PCA, PRA or PBA) were mixed with 50 μL of distilled water and 50 μL Folin-Ciocalteu reagent (Biopack) (1:1). The mixture was stirred and incubated for 3 min. After that, 100 μL of Na<sub>2</sub>CO<sub>3</sub> 20% was added per sample. Finally, distilled water was added to the mixture to final volume of 1500 μL and was incubated at room temperature for 90 min. Absorbance was



**Scheme 1.** A- Extraction protocol of alginate from kelp, with final conversion to sodium alginate. B- Purification protocol of CA, RA and BA alginates.

measure at 760 nm using gallic acid (Sigma-Aldrich) as standard. Results are expressed as mg gallic acid per g of sodium alginate.

### 2.3.6. Protein evaluation

Protein remnants in alginate extracts were determined by electrophoresis. Briefly, 10  $\mu$ l of 1% alginate was seeded on cellulose acetate strips, and the electrophoresis was performed under constant current of 1 mA/cm, using a migration buffer at pH 8.8. After 45 min, the electrophoresis was stopped, and the strips were stained with a Ponceau S solution (Sigma-Aldrich) for 10 min and destained by further washings with 5% acetic acid (Biopack). An evaluation protein present in the band was assessed by visualization in a photography taken with a Nikon camera.

## 2.4. Biocompatibility and cytotoxicity studies

### 2.4.1. Cell cultures and incubations

**2.4.1.1. Bone marrow stromal cells (BMSC).** Bone marrow stromal cells (BMSC) were obtained according to standard procedures in our laboratory [17]. Briefly, animals (*Sprague-Dawley*, 190–210 g), were sacrificed under anesthesia by rapid neck dislocation. BMSC were collected by flushing medullary canal of the dissected femoral and tibial diaphysis, with Dulbecco's Modified Eagle's Medium (DMEM) (Invitrogen, Buenos Aires, Argentina) under sterile conditions. The resulting suspension was seeded in a 25 cm<sup>2</sup> tissue culture flask. Cells were grown in DMEM supplemented with 10% (v/v) Fetal Bovine Serum (FBS) and antibiotics (100 U/ml penicillin and 100 g/ml streptomycin) in a humidified atmosphere of 95% air and 5% CO<sub>2</sub>, at 37 °C. The management of the animals was carried out according to the Guide for the Management and Use of Laboratory Animals [Guidelines on Handling and Training of Laboratory Animals, 1992], under the conditions established in the national bioethical standards - Provision

ANMAT 6677/10 - e international - Nuremberg Code, Helsinki Declaration and its amendments. The protocol to carry out the study in animals was approved by the Comité Institucional para el Cuidado y Uso de Animales de Laboratorio (CICUAL, Protocol No. 019-06-15) of the Faculty of Exact Sciences of the Universidad Nacional de La Plata, Argentina.

For the experiments, unpurified and purified alginate stock concentrated solutions from the three sources (CA, RA and BA) were prepared in distilled water and sterilized by autoclaving. After that, dilutions of the stock alginate solutions were diluted in DMEM-5%FBS to a final concentration of 0.02%.

**2.4.1.2. Cytotoxicity studies.** Murine macrophage RAW 264.7 cells are derived from a cell line established from an ascite-tumor induced by the Abskelon leukemia virus in *Mus musculus*. Its morphology is monocytic, round and adherent [18]. It produces different markers of cytotoxicity, such as interleukin, nitric oxide production (NO) and expression of nitric oxide synthetases (NOS) against toxic substances [19], in addition to morphological changes. For these characteristics, they are considered an excellent model for studies of cytotoxicity of different substances on biological systems. RAW 264.7 cells were grown in basal media (DMEM supplemented with 10% (v/v) FBS and antibiotics (100 U/ml penicillin and 100 g/ml streptomycin)) in a humidified atmosphere of 95% air and 5% CO<sub>2</sub>, at 37 °C.

### 2.4.2. Cell viability

Cell viability was evaluated by the 3-(4,5-dimethylthiazol-2-yl)-2,5-diphenyl tetrazolium bromide (MTT, Sigma) bioassay using RAW 264.7 cells or BMSC. This assay measured the reduction of the tetrazolium salt MTT to formazan by intact mitochondria in living cells. Thus, absorbance change was directly proportional to the number of viable cells. Briefly, 3  $\times$  10<sup>5</sup> cells per well in basal media were seeded on multiwell

culture plates during 24 h in order to allow cell adhesion. Then, media was replaced with different concentrations of alginate sample solution diluted in DMEM and additionally cultured during 48 h. After that, conditioned media was replaced by a solution of 0.1 mg/mL MTT and incubated for additional 1 h. After washing, the formazan precipitate was dissolved in dimethyl sulfoxide (DMSO, Merck) and the absorbance was read at 570 nm.

#### 2.4.3. Biocompatibility studies

BMSC were induced to differentiate into osteoblasts using an osteogenic medium (DMEM–10% FBS containing 25 mg/mL ascorbic acid and 5 mM sodium  $\beta$ -glycerol-phosphate) in the presence of different alginates samples, which were changed every other day. Osteoblastic differentiation was evaluated by measuring alkaline phosphatase activity (ALP) and collagen type 1 production. After 15 days of osteogenic differentiation, cell monolayer was washed with PBS and the total cell extract was obtained with 200  $\mu$ L 0.1% Triton-X100. A 100  $\mu$ L aliquot of the extract was used to evaluate ALP by hydrolysis of *p*-nitrophenylphosphate (p-NPP, Sigma-Aldrich) into *p*-nitrophenol (p-NP) at 37 °C for 1 h. After determined times, the absorbance of p-NP was recorded at 405 nm [20]. Aliquots of each cell extract were used for protein determination by Bradford's technique [21]. Collagen type I production was also determined after 15 days of osteogenic differentiation. Briefly, cells were fixed with Bouin's solution and stained with Sirius red dye for 1 h. The stained material was dissolved in 1 ml 0.1 N sodium hydroxide and the absorbance of the solution was recorded at 550 nm [22].

#### 2.4.4. Cytotoxicity assay

Nitric oxide (NO) production was assessed using Griess reaction [23,24], using sulfanilic acid (Merck) as the diazotating agent and *N*-1-naphthylethylene diamine (Sigma-Aldrich) as the coupling agent. Briefly,  $3 \times 10^5$  RAW 264.7 cells per well in basal media were seeded on multiwell culture plates during 24 h in order to obtain correct adhesion. After that time, culture medium was replaced with alginate solutions diluted in DMEM-5% FBS. NO released was measured after 48 h in the conditioned media. Briefly, 500  $\mu$ L of conditioned media or nitrite (Biopack) standards (0–100 nM) were mixed with 500  $\mu$ L of Griess reagent (1% sulfanilamide and 0.1% naphthylethylene-diamine in 5% phosphoric acid (Merck), and absorbance was measured at 550 nm against a blank prepared with non-conditioned medium. Controls of positive (cells treated with lipopolysaccharide (LPS, 1  $\mu$ g/mL)) and negative (cells without treatment) release of NO were also included.

With the objective to observe morphological changes, RAW264.7 cells were exposed to different alginates. After 48 h of cultured, RAW264.7 monolayer were washed with phosphate-buffered saline (PBS, pH 7.4), fixed with methanol during 5 min and stained with Giemsa. Finally, cells were observed using a Nikon Eclipse TS100 inverted optical microscope.

#### 2.5. Statistical analysis

Results are expressed as mean  $\pm$  SEM and, unless indicated otherwise, were obtained from two separated experiments performed in triplicate. Differences between groups were assessed by one-way ANOVA with Tuckey post hoc test using GraphPad InStat version 3.00 (GraphPad Software).  $p < 0.05$  was considered significant for all statistical analyses.

### 3. Results and discussion

Bone tissue engineering uses different materials, synthetic or natural polymers, to create scaffolds to guide the regeneration of damaged bone. In parallel with the increase in the global life expectancy of general population the frequency of bone-related diseases (fracture due

to osteoporosis, osteonecrosis, etc.) is increasing [25,26]. Under these patho-physiological conditions or extended damage, bone repair is limited. For this reason, it is of great importance to develop new scaffolds that can be used to repair damaged bone. On the other hand, ideally the source of the biomaterial should be derived from renewable sources with a minimum impact on the environment, and it would be economically affordable. Based on these premises, we isolated and studied alginate, a natural polymer obtained from *Undaria pinnatifida*.

#### 3.1. Physico-chemical characterization

The extraction yield of sodium alginate obtained from blade and midrib of *Undaria pinnatifida* was 12% and 17% (g sodium alginate/g seaweed), respectively. Under our experimental conditions, the yield of the extraction was similar to that obtained by Apoya et al. [7], but it was not comparable to those obtained by Skriptsova et al. [27]. This difference could be attributed to the different extraction protocol used by these last authors, but it also could be a consequence of geographical variations in alginate production by the seaweed itself.

It has been previously reported that both commercial and isolated from *Undaria pinnatifida* alginates present impurities that may affect their biological properties. Thus, we have purified both alginate samples in order to reduce or eliminate possible impurities. We used the Sevag's purification protocol, after which the purification yield was 68% 55% and 45% for CA, RA and BA respectively, calculated as g sodium alginate purified/g sodium alginate unpurified. After that, the characterization of the purified alginates was carried out using FTIR, TGA,  $^1\text{H-RMN}$ , and a viscosity.

The assignments of different FTIR signals were performed according to Madhusudana Rao [28]: FTIR (thin film,  $\text{cm}^{-1}$ ): 3430 (O-H); 2930 (C-H); 1610, 1415 and 1306 were attributed to stretching vibrations of asymmetric and symmetric bands ( $\text{COO}^-$ ). These bands could be assigned to the characteristic functional groups of the polysaccharides present in all the samples studied.

We also evaluated the thermal behavior of both purified and non-purified samples through thermogravimetric analysis (TGA) under  $\text{N}_2$  atmosphere (Fig. 1), and the relevant decomposition temperatures data calculated from that graphic is shown in Table 1. At the beginning of thermal degradation (before 150 °C), it was observed a loss of mass, which could be attributed to moisture or coordination water (Fig. 1). Then, two markedly different decomposition stages occurred: the first one between 200 and 600 °C and the second one from 600 °C. According to other authors' observations, these decomposition stages could correspond to sodium alginate thermal dehydration, followed by formation and degradation of  $\text{Na}_2\text{CO}_3$ , respectively (Fig. 1) [29,30].

Initial decomposition temperatures (IDT) were similar and close to 200 °C for all sodium alginates studied independent of their origin or purification state (Table 1).  $T_{\text{max}1}$  and  $T_{\text{max}2}$  are the maximum decomposition temperatures for each decomposition stage. While  $T_{\text{max}1}$  did not change with purification process,  $T_{\text{max}2}$  showed a shift to higher temperatures and represented a higher loss of mass (value in parentheses). Consistently, it was observed a decrease in the amount of the residue after purification. With TGA studies we concluded that the initial decomposition temperatures of sodium alginate were not affected by purification process.

The structural characterization of the samples was analyzed by  $^1\text{H}$  NMR, and the copolymer composition was determined by anomeric protons region evaluation as it was previously reported [14]. The following assignments were used to get the integral ratios (I) from Fig. 2: glucuronic acid anomeric proton at 5.03 ppm ( $I_{\text{GAA}}$ ); mannuronic acid anomeric proton at 4.64 ppm ( $I_{\text{MAA}}$ ); 5H guluronic acid at 4.41 ppm ( $I_{\text{GA}}$ ). The molar fraction (F) of each monomer (G or M) in the copolymer was calculated by using the equation presented in Table 2:

All samples had a similar quantity of both monomers in their structure characterized by the  $F_{\text{M}}$  and  $F_{\text{G}}$  value (Table 2). These results are in concordance to those reported by other authors [31].



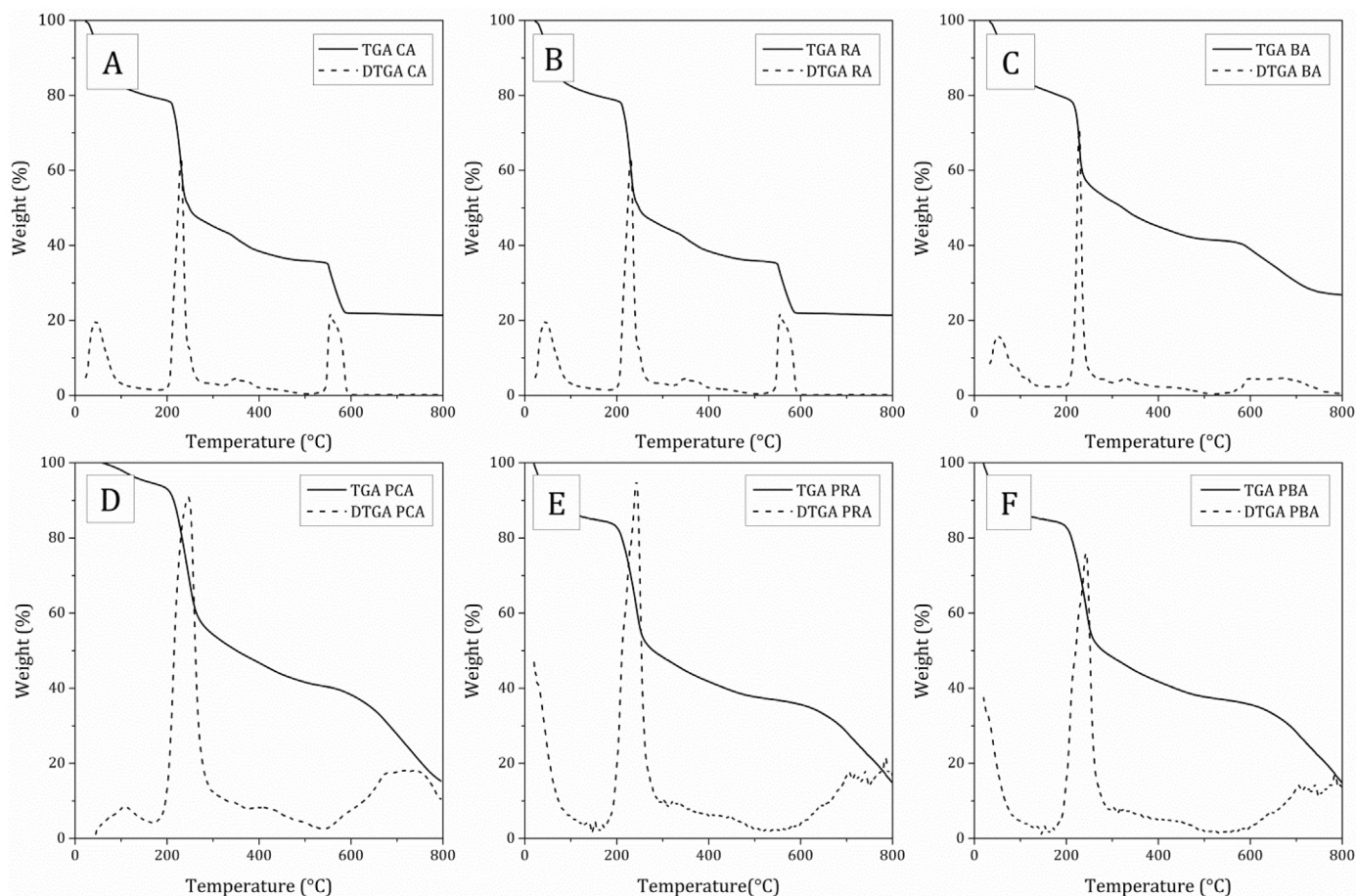


Fig. 1. Thermal stability of CA [A], RA [B], BA [C], PCA [D], PRA [E] and PBA [F].

Table 1

TGA data for Commercial Alginate (CA), Purified Commercial Alginate (PCA), Midrib Alginate (RA), Purified Midrib Alginate (PRA), Blade Alginate (BA) and Purified Blade Alginate (PBA).

Sample	IDT (°C)	T <sub>max1</sub> <sup>a</sup> (°C)	T <sub>max2</sub> <sup>a</sup> (°C)	Residue % 800 °C
CA	207.5	230.2 (40.0)	560.7 (71.8)	20
PCA	205.6	246.1 (29.1)	718.5 (75.1)	15
RA	209.8	228.0 (31.9)	653.7 (65.9)	27
PRA	201.8	243.7 (38.5)	748.9 (77.0)	14
BA	204.5	235.5 (29.6)	697.6 (59.1)	34
PBA	203.8	242.8 (33.8)	702.8 (77.8)	12

<sup>a</sup> Value in parentheses indicates the percentage of total mass lost (%) up to the stated temperature.

Table 2

Composition NMR data for all samples.

Sample	$F_G = \frac{I_{GAA}}{I_{MAA} + I_{GA}}$	$F_M = 1 - F_G$	$\frac{M/G}{F_G} = \frac{1 - F_G}{F_G}$	$M_v$ (g/mol) × 10 <sup>5</sup>
CA	0.50	0.50	1.05	3.5
PCA	0.43	0.57	1.43	2.9
RA	0.50	0.50	1.00	2.9
PRA	0.45	0.55	1.23	1.8
BA	0.55	0.45	0.84	2.4
PBA	0.41	0.59	1.44	1.5

The NMR analysis also showed that the purification process generated a slight change in the polymer composition in accordance with the peaks shape (Fig. 2). These observations suggested a change in the structure of the polysaccharide after the purification process that it had

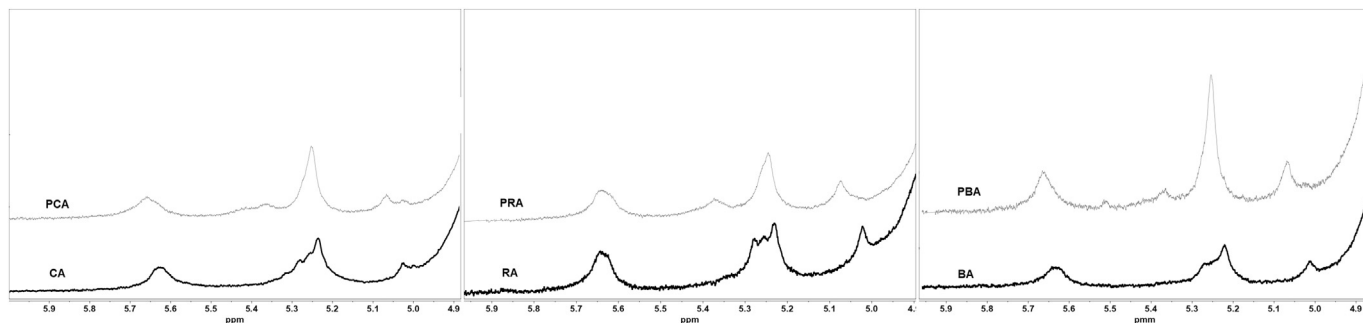
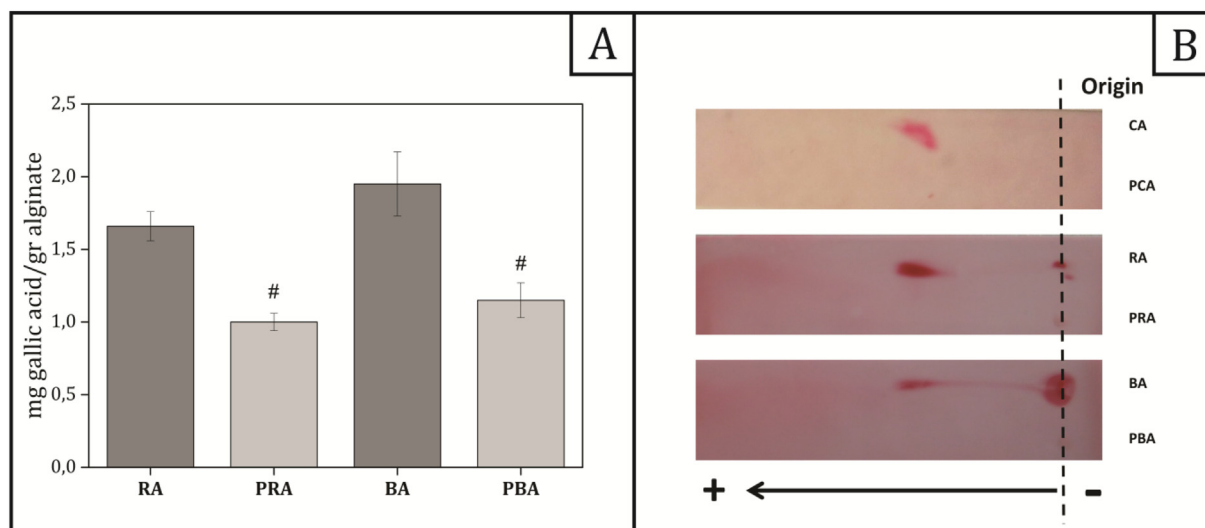
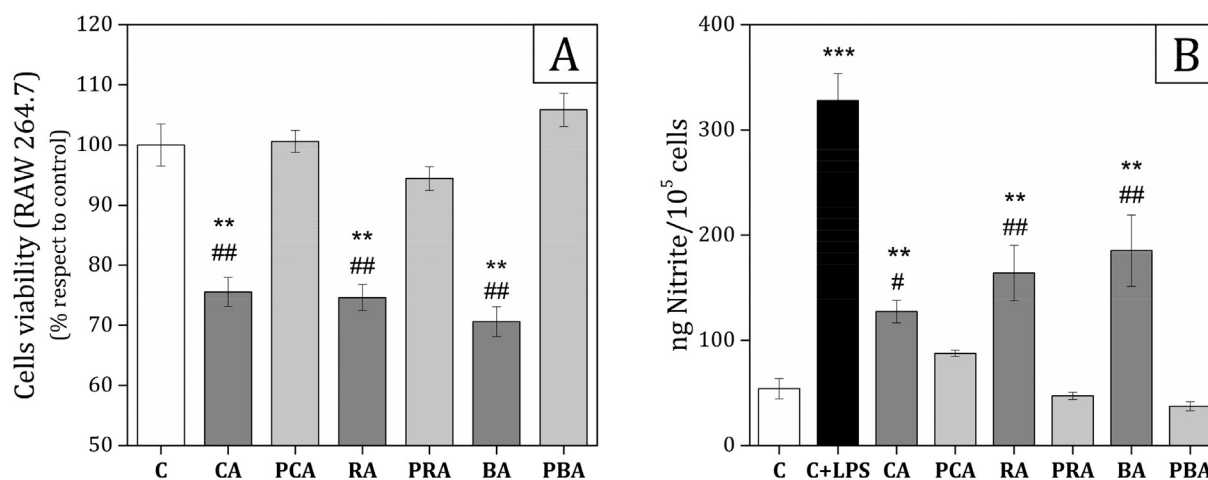


Fig. 2. <sup>1</sup>H NMR spectrum for all unpurified (CA, RA and BA) and purified (PCA, PRA and PBA) polysaccharides samples.



**Fig. 3.** Evaluation of the impurities presents in the alginate samples, before (RA, BA and CA) and after (PRA, PBA and PBA) purification step. [A] Polyphenols determination in RA, PRA, BA and PBA. Data are expressed as mean  $\pm$  SEM,  $n = 4$ . Differences are #:  $p < 0.05$  vs unpurified alginate. [B] Semiquantitative protein determination by electrophoresis in strips of cellulose acetate of CA, PCA, RA, PRA, BA and PBA.



**Fig. 4.** Cytotoxicity studies. [A] RAW 264.7 cell viability and [B] NO production after 48 h of incubation with sodium alginates. Data are expressed as mean  $\pm$  SEM,  $n = 9$  for both A and B. Differences are: \*:  $p < 0.05$  vs cell culture-plate control (C); \*\*:  $p < 0.01$  vs. C; \*\*\*:  $p < 0.001$ ; #:  $p < 0.05$  vs. purified alginate, ##:  $p < 0.01$  vs. purified alginate.

not been studied in depth since they exceeded the objective of this work.

In addition, the Table 2 shows viscosity average molecular weight ( $M_v$ ) value for each sample determined by capillary viscosity. The intrinsic viscosity ( $[\eta]$ ) was calculated from double extrapolation of the Huggins and Kramer equations:

$$\frac{\eta_{sp}}{c} = [\eta] + k_H [\eta]^2 c \quad (1)$$

$$\frac{\ln \eta_r}{c} = [\eta] + k_K [\eta]^2 c \quad (2)$$

where  $\eta_r$  is the relative viscosity,  $\eta_{sp}$  is the specific viscosity,  $k_H$  and  $k_K$  are the Huggins and Kramer coefficients, respectively.  $[\eta]$  was estimated as the average of the two ordinate intercepts from the two extrapolations (graphics not shown). The viscosity average molecular weight was determined using Mark-Huggins equation:

$$[\eta] = kM_v^a \quad (3)$$

where  $K$  and  $a$  are Mark-Huggins constants, and they were obtained from literature [15]. As it can be seen in Table 2, the  $M_v$  values after

purification decreased and the viscosimetric molecular weight for sodium alginate extracted from seaweed was lower than that of the polysaccharide from commercial origin.

The main impurities present in alginate, regardless of the origin, are polyphenols, proteins and endotoxins, and they could limit the use of this polymer in Bone Tissue Engineering (BTE). In this work, we have evaluated the polyphenols and protein content in sodium alginate samples before (RA and BA) and after (PRA and PBA) the purification process through the Folin-Ciocalteu method (Fig. 3A) and electrophoresis in cellulose/acetate strips (Fig. 3B), respectively.

After purification procedure, the content of polyphenols decreased by approximately 60% in RA and BA samples (#:  $p < 0.05$  compared to purified alginate). While in non-purified commercial alginate samples, polyphenols were under detection limits. The results show that it is necessary to carry out a purification process because the pre-extraction process with formaldehyde does not completely eliminate the polyphenols in the samples. On the other hand, in Fig. 3B it can be observed high levels of protein impurities in unpurified alginates, which were not detected after the purification procedure. Our results are in agreement with previous reports [9,32] describing high levels of

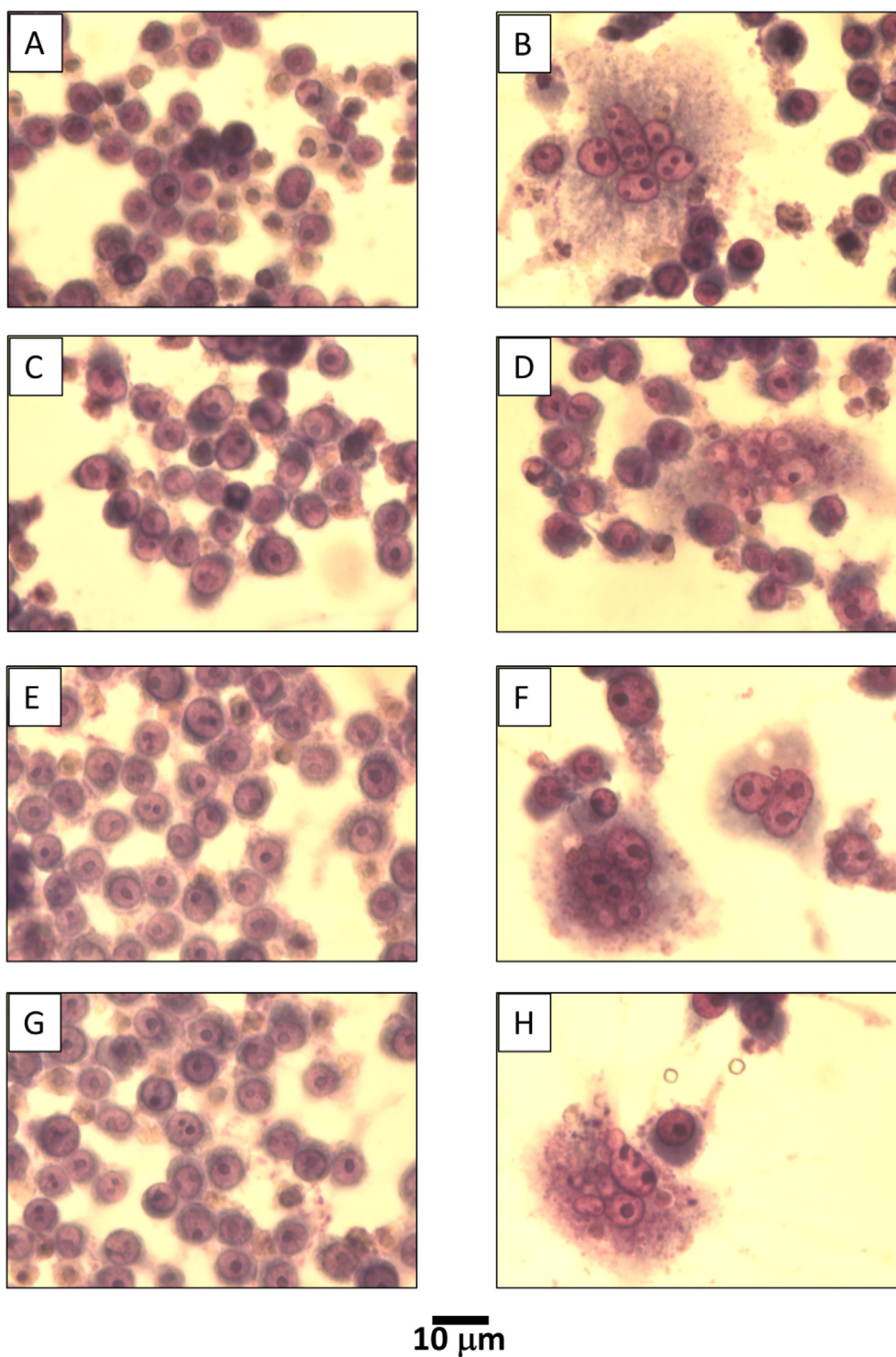


**Fig. 5.** RAW 264.7 cell morphology. Cell were stained with Giemsa after 48 h of culture in cell culture-plates, control [A]; LPS as positive controls of cytotoxic [B]; PCA [C]; CA [D]; PRA [E]; RA [F]; PBA [G] and BA [H]. Photograph shows a representative field of cells cultures under each condition. Magnification 400 $\times$ .

both polyphenols and proteins, as major contaminants of unpurified alginates. However, we demonstrated that the introduction of a simple purification step leads to almost elimination of these contaminants. In concordance, the low percentage of final mass achieved in the thermogravimetric analysis indicated a decrease in the content of salts, and globally suggested a decrease on impurities in the samples (Table 1).

### 3.2. Biocompatibility and cytotoxicity studies

The materials candidates to be used in BTE must have low or no cytotoxicity. Macrophages RAW 264.7 are a well-known and sensitive model to evaluate in vitro cytotoxicity, and it has been extensively used to evaluate toxicity of the biomaterials [19,33–36]. In the present work, we used this culture model to evaluate the toxic effect, if any, of the different alginates samples before and after purification (Fig. 4).

We found that RAW264.7 cell viability decreased in the presence of

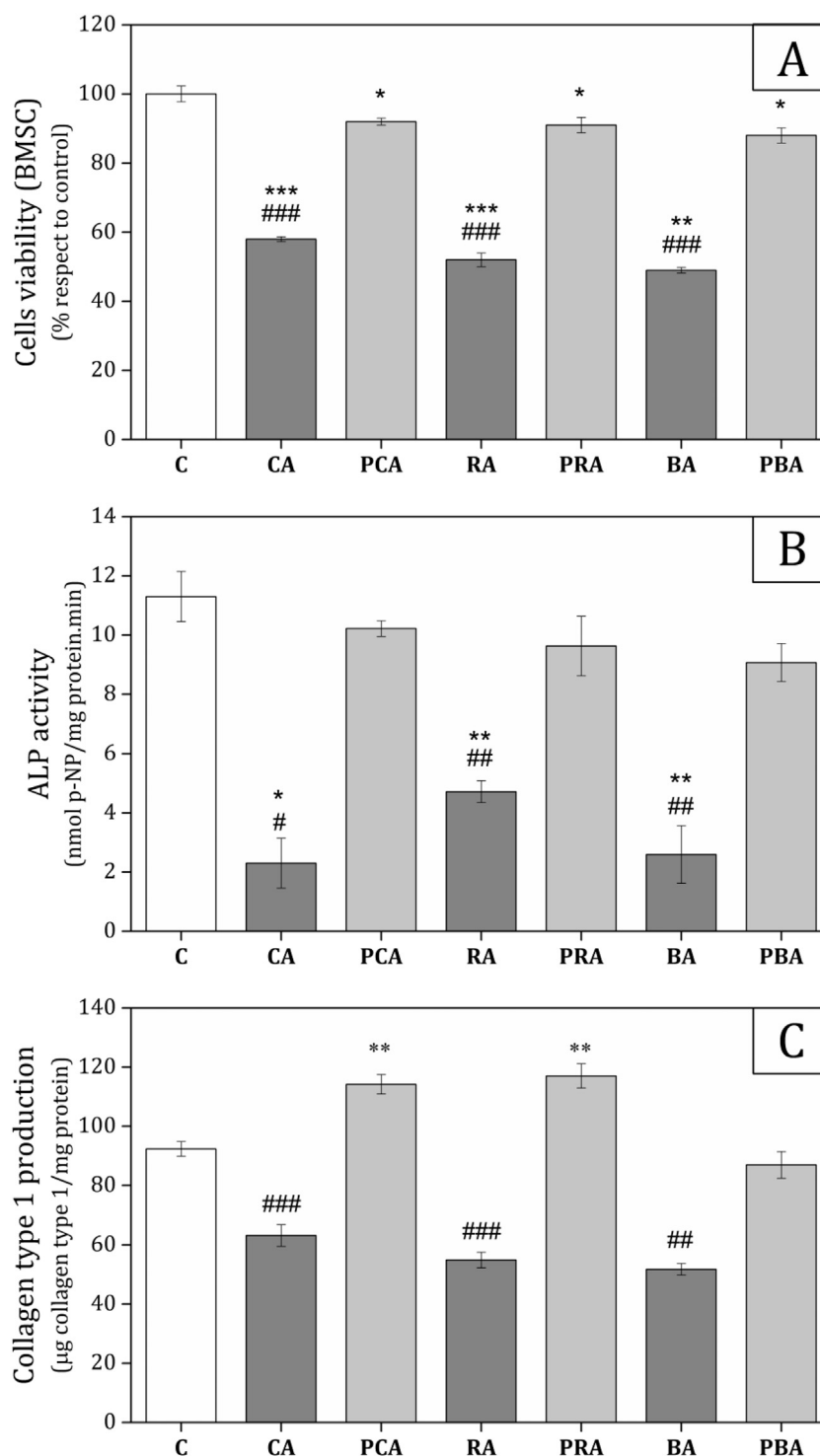


**Fig. 6.** Biocompatibility of alginates for bone marrow mesenchyme cells (BMSC). Cells were cultured with or without sodium alginates purified (PCA, PBA and PRA) or unpurified (CA, BA and RA), for 48 h under basal conditions to evaluate cells viability (A) or with osteoblastic differentiation media for 14d to determine ALP activity (B) and type 1 collagen production (C). Results are expressed as mean  $\pm$  SEM, for  $n = 7$  (A),  $n = 4$  (B) and  $n = 8$  (C). Differences are: \*;  $p < 0.05$  vs dish culture control (C); \*\*:  $p < 0.01$  vs. C; \*\*\*:  $p < 0.001$ ; #:  $p < 0.05$  vs. purified alginate, ##:  $p < 0.01$  vs. purified alginate and ###:  $p < 0.001$  vs. purified alginate.

unpurified alginate (CA, RA and BA) after 48 h of culture (\*\*:  $p < 0.01$  respect to control), an effect that it was prevented by purification of the alginate samples (Fig. 5A, PCA, PRA and PBA). In accordance, the addition of unpurified alginate to RAW264.7 cells culture stimulated NO release respect to control condition (Fig. 5B, \*\*:  $p < 0.01$ ), while purified alginate had no effect. Altogether, our results suggested that the impurities present in the extracts of alginates induced a toxic effect

that could be avoided by a simple purification step.

Additionally, we have studied RAW264.7 cell morphology as another evidence of cytotoxicity. We found that cells growing in standard tissue culture dishes showed a rounded morphology with few cytoplasmic extensions (Fig. 5A). While after the addition of unpurified alginates, the cells presented an expanded and vacuolated cytoplasm with several cytoplasmic extensions, suggesting activation of the



macrophages (Fig. 5D, F and H). Similar alterations of cell morphology were observed when cells growing on tissue culture dish were exposed to LPS, as a positive control of cytotoxicity (Fig. 5B). However, after purification alginates induced no change on cell morphology, suggesting no or low cytotoxicity (Fig. 5C, E and G). Similar alterations were observed by other authors, as well as an increase on different pro-inflammatory cytokines [37,38]. Moreover, it has been demonstrated that there is a relationship between alginate oligosaccharides and cytokines production by RAW264.7; as well as it was also reported that alginate can be phagocytosed by RAW by increasing p38 MAPs signaling pathways which in turn could stimulate the cytokine release [38,39]. However, in our study, the observed cytotoxic effect could be attributed almost exclusively to the presence of impurities, since it disappeared after the purification process.

Since we were interested in the development of biomaterials for BTE, we also studied the biocompatibility of alginates from different sources, and their purified derivatives, using bone marrow stromal cells (BMSC). This cell type is present in the proximity of endosteum and it is recruited after bone tissue lesions to restore the damage, since they have the capacity to proliferate and differentiate to osteoblastic lineage. In the present work, we have evaluated the ability of alginates, purified or unpurified, to support BMSC viability and osteoblastic differentiation. As it is shown in Fig. 6A, BMSC viability considerably decreased when cells were incubated in the presence of unpurified alginate (CA, BA, RA) in comparison with BMSC cells growing on standard tissue culture plates (\*\*\*:  $p < 0.001$  vs. the control). Similarly, other authors have also reported a decrease on osteoblastic - related cell viability using commercial alginates [32,40–42]. These authors did not use any further purification of the alginate samples, suggesting once again that the impurities presents in the samples could cause the toxic effect. Moreover, we found that the toxic effect of alginates on BMSC proliferation was almost completely diminished after purification step when cells were exposed to alginates up to 48 h.

Then, we evaluated the capacity of BMSC growing in the presence of alginate to differentiate to bone forming cells. We found that ALP activity and type 1 collagen deposition decreased when cells were cultured with unpurified alginates (Fig. 6B and C respectively; CA, RA and BA bars), an effect that was reverted by alginate purification (Fig. 6B and C, respectively; PCA, PRA and PBA bars). In this way, we observed that although cell viability was not totally recovered at the control level, it was necessary to carry out the purification process of the alginates in order to obtain an adequate environment for osteoblastic differentiation without an inflammatory response.

#### 4. Conclusion

In conclusion, we isolated, characterized and in vitro evaluated the biocompatibility and cytotoxicity of sodium alginates from midrib and blade of *Undaria pinnatifida*. We have observed that these alginates possessed impurities, such as polyphenols and proteins, that caused a toxic effect in RAW264.7, while avoided BSMC proliferation and osteoblastic differentiation. We also demonstrated that a simple purification step decreased impurities to such low levels that the toxic effect was reversed and the biocompatibility was improved, without producing relevant changes in the sodium alginate physicochemical characteristics. Therefore, we have shown that it is necessary to carry out a purification process to obtain biocompatible alginates with low toxicity, suitable for bone tissue engineering.

#### Acknowledgments

This work was partially supported by grants from Facultad de Ciencias Exactas, Universidad Nacional de La Plata (UNLP), Comisión de Investigaciones Científicas de la Provincia de Buenos Aires (CICPBA) and Agencia Nacional de Promoción Científica y Tecnológica (PICT 2015-1030). MLT is a fellow of CONICET, JMF, TGO and FGD are a

member of the Carrera del Investigador of CONICET, and AMC is a member of the Carrera del Investigador Científico de la CICPBA.

#### Author contributions

ML Torres, performed the experiments, analyzed and interpreted the data. JM Fernandez, AM Cortizo, designed and supervised biology experiments, wrote and discussed the article. FG Dellatorre, provided the raw material from *Undaria pinnatifida* and wrote the article. TG Oberti, designed and supervised physicochemical experiments, wrote and discussed the article.

#### Conflict of interest statement

The authors declare no conflict of interest.

#### Statement of informed consent, human/animal rights

All experiments with animals were performed in conformity with the Guidelines on Handling and Training of Laboratory Animals published by the Universities Federation for Animals Welfare (Guide of TCaUoLA, 2011). Approval for animal studies was obtained from the institutional animal care committee (CICUAL approval number: 001–05-15). Animals were sacrificed by cervical dislocation under anesthesia and femora and tibia were dissected.

#### Declaration of authors

All the participants share authorship of this work and agree to submit the manuscript for peer review to Algal Research.

#### References

- [1] A.J. Salgado, O.P. Coutinho, R.L. Reis, Bone tissue engineering: state of the art and future trends, *Macromol. Biosci.* 4 (2004) 743–765, <https://doi.org/10.1002/mabi.200400026>.
- [2] G. Wei, P.X. Ma, Structure and properties of nano-hydroxyapatite/polymer composite scaffolds for bone tissue engineering, *Biomaterials* 25 (2004) 4749–4757, <https://doi.org/10.1016/j.biomaterials.2003.12.005>.
- [3] X. Liu, P.X. Ma, Polymeric scaffolds for bone tissue engineering, *Ann. Biomed. Eng.* 32 (2004) 477–486 <http://www.ncbi.nlm.nih.gov/pubmed/15095822>, Accessed date: 16 April 2018.
- [4] R. Langer, J.P. Vacanti, Tissue engineering, *Science* 260 (1993) 920–926 <http://www.ncbi.nlm.nih.gov/pubmed/8493529>, Accessed date: 16 April 2018.
- [5] S. Stratton, N.B. Shelke, K. Hoshino, S. Rudraiah, S.G. Kumbar, Bioactive polymeric scaffolds for tissue engineering, *Bioact. Mater.* 1 (2016) 93–108, <https://doi.org/10.1016/j.bioactmat.2016.11.001>.
- [6] F. Dellatorre, R. Amoroso, J. Saravia, L. Orensanz, Rapid expansion and potential range of the invasive kelp *Undaria pinnatifida* in the Southwest Atlantic, *Aquat. Invasions* 9 (2014) 467–478, <https://doi.org/10.3391/ai.2014.9.4.05>.
- [7] M. Apoya, H. Ogawa, N. Nanba, Alginate content of farmed *Undaria pinnatifida* (Harvey) Suringar from the three bays of Iwate, Japan during harvest period, *Bot. Mar.* 45 (2002) 445–452, <https://doi.org/10.1515/BOT.2002.045>.
- [8] F.G. Dellatorre, R. Amoroso, P.J. Barón, El alga exótica *Undaria pinnatifida* en Argentina: biología, distribución y potenciales impactos, Editorial Académica Española, 2012.
- [9] J. Dusseault, S.K. Tam, M. Ménard, S. Polizu, G. Jourdan, L. Yahia, J.-P. Hallé, Evaluation of alginate purification methods: effect on polyphenol, endotoxin, and protein contamination, *J. Biomed. Mater. Res. Part A* 76A (2006) 243–251, <https://doi.org/10.1002/jbm.a.30541>.
- [10] S.L. Holdt, S. Kraan, Bioactive compounds in seaweed: functional food applications and legislation, *J. Appl. Phycol.* 23 (2011) 543–597, <https://doi.org/10.1007/s10811-010-9632-5>.
- [11] D. Arvizu-Higuera, Optimización del proceso de extracción de alginato de sodio, a partir del alga café *Macrocystis pyrifera*, Instituto Politécnico Nacional, CICIMAR, 1993.
- [12] L.B. Yusha IQ, L. Lu, C. Zhou, Purification of Alginate for Tissue Engineering, *IEEE*, 2009, pp. 1–4.
- [13] Roy Lester Whistler, *Methods in Carbohydrate Chemistry/Vol. 5, General Polysaccharides*, Academic Press, New York, 1965.
- [14] M. Fertah, A. Belfkira, E. montassir Dahmane, M. Taourirte, F. Brouillette, Extraction and characterization of sodium alginate from Moroccan *Laminaria digitata* brown seaweed, *Arab. J. Chem.* 10 (2017) S3707–S3714, <https://doi.org/10.1016/J.ARABJC.2014.05.003>.
- [15] B.T. Stokke, K.I. Draget, O. Smidsrød, Y. Yuguchi, H. Urakawa, K. Kajiwara, Small-

- angle X-ray scattering and rheological characterization of alginate gels. 1. Ca-alginate gels, *Macromolecules* (2000) 1853–1863, <https://doi.org/10.1021/ma991559q>.
- [16] V.L. Singleton, R. Orthofer, R.M. Lamuela-Raventós, [14] Analysis of total phenols and other oxidation substrates and antioxidants by means of folin-ciocalteu reagent, *Methods Enzymol.* 299 (1999) 152–178, [https://doi.org/10.1016/S0076-6879\(99\)99017-1](https://doi.org/10.1016/S0076-6879(99)99017-1).
- [17] M.S. Molinuevo, L. Schurman, A.D. McCarthy, A.M. Cortizo, M.J. Tolosa, M.V. Gangoi, V. Arnol, C. Sedlinsky, Effect of metformin on bone marrow progenitor cell differentiation: in vivo and in vitro studies, *J. Bone Miner. Res.* 25 (2010) 211–221, <https://doi.org/10.1359/jbmr.090732>.
- [18] W.C. Raschke, S. Baird, P. Ralph, I. Nakoinz, Functional macrophage cell lines transformed by Abelson leukemia virus, *Cell* 15 (1978) 261–267 <http://www.ncbi.nlm.nih.gov/pubmed/212198>, Accessed date: 17 April 2018.
- [19] L.C. Denlinger, P.L. Fiset, K.A. Garis, G. Kwon, A. Vazquez-Torres, A.D. Simon, B. Nguyen, R.A. Proctor, P.J. Bertics, J.A. Corbett, Regulation of inducible nitric oxide synthase expression by macrophage purinoreceptors and calcium, *J. Biol. Chem.* 271 (1996) 337–342 <http://www.ncbi.nlm.nih.gov/pubmed/8550583>, Accessed date: 17 April 2018.
- [20] A.M. Cortizo, S.B. Etcheverry, Vanadium derivatives act as growth factor? Mimetic compounds upon differentiation and proliferation of osteoblast-like UMR106 cells, *Mol. Cell. Biochem.* 145 (1995) 97–102, <https://doi.org/10.1007/BF00935481>.
- [21] M.M. Bradford, A rapid and sensitive method for the quantitation of microgram quantities of protein utilizing the principle of protein-dye binding, *Anal. Biochem.* 72 (1976) 248–254, [https://doi.org/10.1016/0003-2697\(76\)90527-3](https://doi.org/10.1016/0003-2697(76)90527-3).
- [22] J.M. Fernandez, M.S. Molinuevo, M.S. Cortizo, A.M. Cortizo, Development of an osteoconductive PCL-PDIPF-hydroxyapatite composite scaffold for bone tissue engineering, *J. Tissue Eng. Regen. Med.* 5 (2011) e126–e135, <https://doi.org/10.1002/term.394>.
- [23] A.M. Cortizo, M. Caporossi, G. Lettieri, S.B. Etcheverry, L. Plata, Vanadate-induced nitric oxide production: role in osteoblast growth and differentiation, *Eur. J. Pharmacol.* 400 (2000) 279–285 [www.elsevier.nl/locate/jep](http://www.elsevier.nl/locate/jep), Accessed date: 17 April 2018.
- [24] M.S. Molinuevo, S.B. Etcheverry, A.M. Cortizo, Macrophage activation by a vanadyl-aspirin complex is dependent on L-type calcium channel and the generation of nitric oxide, *Toxicology* 210 (2005) 205–212, <https://doi.org/10.1016/j.tox.2005.02.016>.
- [25] A.R. Amini, C.T. Laurencin, S.P. Nukavarapu, Bone tissue engineering: recent advances and challenges, *Crit. Rev. Biomed. Eng.* 40 (2012) 363–408 <http://www.ncbi.nlm.nih.gov/pubmed/23339648>, Accessed date: 17 April 2018.
- [26] B. Baroli, From natural bone grafts to tissue engineering therapeutics: brainstorming on pharmaceutical formulative requirements and challenges, *J. Pharm. Sci.* 98 (2009) 1317–1375, <https://doi.org/10.1002/jps.21528>.
- [27] A. Skriptsova, V. Khomenko, V. Isakov, Seasonal changes in growth rate, morphology and alginate content in *Undaria pinnatifida* at the northern limit in the Sea of Japan (Russia), *J. Appl. Phycol.* 16 (2004) 17–21, <https://doi.org/10.1023/B:JAPH.0000019049.74140.61>.
- [28] K. Madhusudana Rao, K.S.V. Krishna Rao, P. Sudhakar, K. Chowdaji Rao, M.C.S. Subha, *J. Appl. Pharm. Sci.* 3 (2013) 061–069 [http://www.japsonline.com/abstract.php?article\\_id=924](http://www.japsonline.com/abstract.php?article_id=924), Accessed date: 17 April 2018.
- [29] Y. Liu, C.-J. Zhang, J.-C. Zhao, Y. Guo, P. Zhu, D.-Y. Wang, Bio-based barium alginate film: preparation, flame retardancy and thermal degradation behavior, *Carbohydr. Polym.* 139 (2016) 106–114, <https://doi.org/10.1016/j.carbpol.2015.12.044>.
- [30] J.P. Soares, J.E. Santos, G.O. Chierice, E.T.G. Cavalheiro, Thermal Behavior of Alginic Acid and Its Sodium Salt, vol. 29, (2004), pp. 53–56 [www.scielo.br/eq](http://www.scielo.br/eq), Accessed date: 17 April 2018.
- [31] T.A. Fenoradosa, G. Ali, C. Delattre, C. Laroche, E. Petit, A. Wadouachi, P. Michaud, Extraction and characterization of an alginate from the brown seaweed *Sargassum turbinarioides* Grunow, *J. Appl. Phycol.* 22 (2010) 131–137 <https://www.cabdirect.org/cabdirect/abstract/20103142073> (accessed April 17, 2018).
- [32] L. Wang, R.M. Shelton, P.R. Cooper, M. Lawson, J.T. Triffitt, J.E. Barralet, Evaluation of sodium alginate for bone marrow cell tissue engineering, *Biomaterials* 24 (2003) 3475–3481 <http://www.ncbi.nlm.nih.gov/pubmed/12809776>, Accessed date: 17 April 2018.
- [33] A.M. Cortizo, G. Ruderman, G. Correa, I.G. Mogilner, E.J. Tolosa, Effect of surface topography of collagen scaffolds on cytotoxicity and osteoblast differentiation, *J. Biomater. Tissue Eng.* 2 (2012) 125–132, <https://doi.org/10.1166/jbt.2012.1039>.
- [34] J.M. Fernández, M.S. Cortizo, A.M. Cortizo, Fumarate/ceramic composite based scaffolds for tissue engineering: evaluation of hydrophilicity, degradability, toxicity and biocompatibility, *J. Biomater. Tissue Eng.* 4 (2014) 227–234, <https://doi.org/10.1166/jbt.2014.1158>.
- [35] J. Bixby, T. Ray, F. Chan, TNF, cell death and inflammation, *Curr. Med. Chem. Anti-Inflamm. Anti-Allergy Agents* 4 (2005) 557–567, <https://doi.org/10.2174/156801405774933214>.
- [36] M. Blonska, Z.P. Czuba, W. Krol, Effect of flavone derivatives on interleukin-1beta (IL-1beta) mRNA expression and IL-1beta protein synthesis in stimulated RAW 264.7 macrophages, *Scand. J. Immunol.* 57 (2003) 162–166, <https://doi.org/10.1046/j.1365-3083.2003.01213.x>.
- [37] M. Kurachi, T. Nakashima, K. Yamaguchi, T. Oda, C. Miyajima, Y. Iwamoto, T. Muramatsu, T. Nakashima, Comparison of the activities of various alginates to induce TNF- $\alpha$  secretion in RAW264.7 cells, *J. Infect. Chemother.* 11 (2005) 199–203, <https://doi.org/10.1007/s10156-005-0392-0>.
- [38] M. Iwamoto, M. Kurachi, T. Nakashima, D. Kim, K. Yamaguchi, T. Oda, Y. Iwamoto, T. Muramatsu, Structure-activity relationship of alginate oligosaccharides in the induction of cytokine production from RAW264.7 cells, *FEBS Lett.* 579 (2005) 4423–4429, <https://doi.org/10.1016/j.febslet.2005.07.007>.
- [39] D. Bi, R. Zhou, N. Cai, Q. Lai, Q. Han, Y. Peng, Z. Jiang, Z. Tang, J. Lu, W. Bao, H. Xu, X. Xu, Alginate enhances Toll-like receptor 4-mediated phagocytosis by murine RAW264.7 macrophages, *Int. J. Biol. Macromol.* 105 (2017) 1446–1454, <https://doi.org/10.1016/j.ijbiomac.2017.07.129>.
- [40] J.F.A. Valente, T.A.M. Valente, P. Alves, P. Ferreira, A. Silva, I.J. Correia, Alginate based scaffolds for bone tissue engineering, *Mater. Sci. Eng. C* 32 (2012) 2596–2603, <https://doi.org/10.1016/j.MSEC.2012.08.001>.
- [41] S. Srinivasan, R. Jayasree, K.P. Chennazhi, S.V. Nair, R. Jayakumar, Biocompatible alginate/nano bioactive glass ceramic composite scaffolds for periodontal tissue regeneration, *Carbohydr. Polym.* 87 (2012) 274–283, <https://doi.org/10.1016/j.carbpol.2011.07.058>.
- [42] D.C. Furuya, S.A. da Costa, R.C. de Oliveira, H.G. Ferraz, A. Pessoa Junior, S.M. da Costa, Fibers obtained from alginate, chitosan and hybrid used in the development of scaffolds, *Mater. Res.* 20 (2017) 377–386, <https://doi.org/10.1590/1980-5373-mr-2016-0509>.